

PNAS

www.pnas.org

Supplementary Information for

An apoptosis-dependent checkpoint for autoimmunity in memory B and plasma cells.

Christian T. Mayer, Jan P. Nieke, Anna Gazumyan, Melissa Cipolla, Qiao Wang, Thiago Y. Oliveira, Victor Ramos, Sébastien Monette, Quan-Zhen Li, M. Eric Gershwin, Hamid Kashkar and Michel C. Nussenzweig

Corresponding authors: Michel C. Nussenzweig; Christian T. Mayer

Email: nussen@rockefeller.edu

christian.mayer@nih.gov

This PDF file includes:

Figures S1 to S4

Legends for Datasets S1 to S3

Other supplementary materials for this manuscript include the following:

Datasets S1 to S3

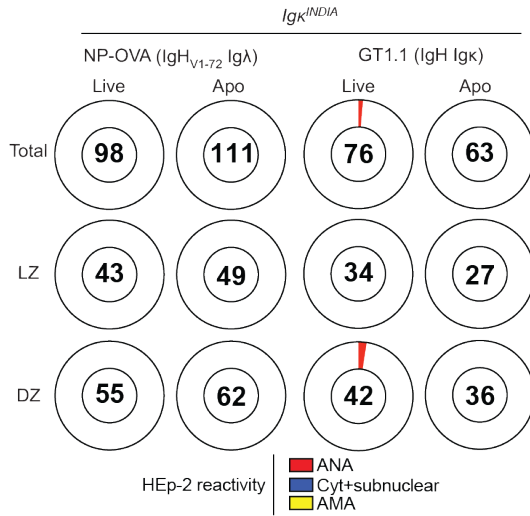
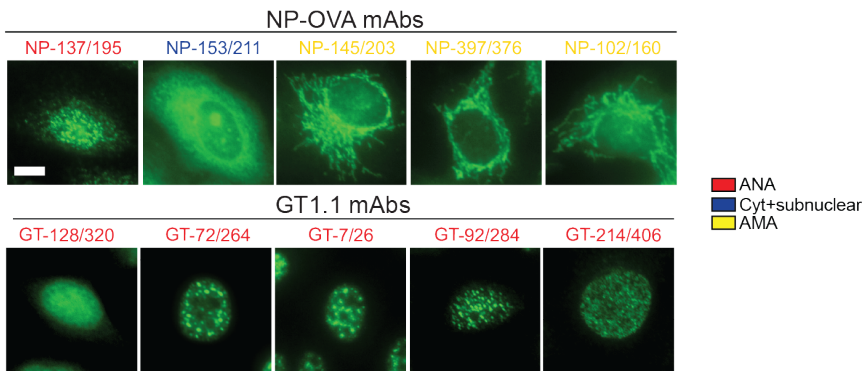
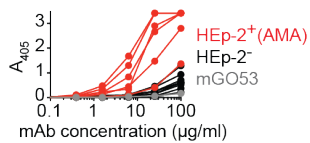
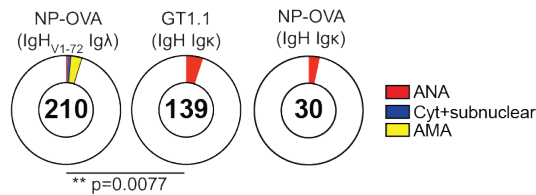
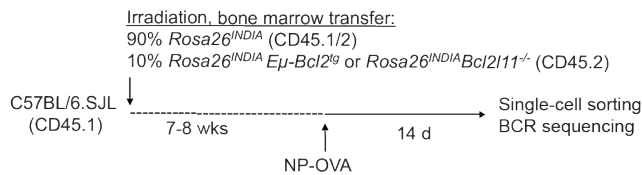
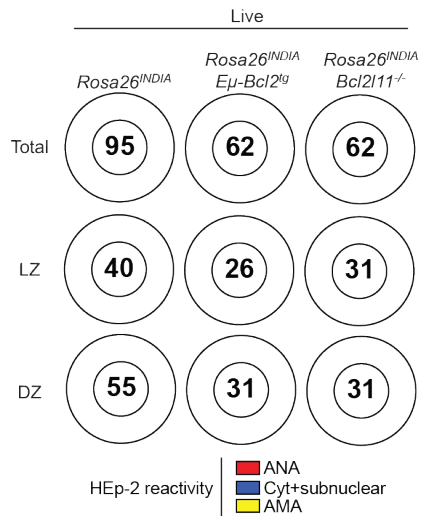
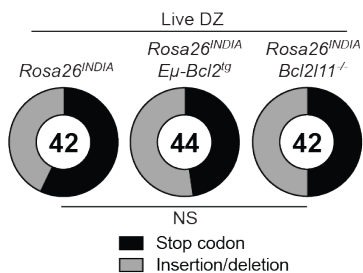
A**B****C****D****E****F****G**

Fig. S1. Autoreactivity in GC B cells

(A-D) *Igk^{NDIA}* mice were immunized with NP-OVA or an HIV-1 envelope protein (GT1.1) followed by single-cell sorting of FRET⁺ (live) and FRET⁻ (apoptotic) DZ and LZ GC B cells, IgH/IgL PCR amplification, cloning and recombinant antibody expression. (A) Same as Fig. 1A but HEp-2 reactive antibodies were tested at 1 µg/ml. (B) HEp-2 fluorescence patterns of monoclonal antibodies showing HEp-2 reactivity at 100 µg/ml (scale bar, 10 µm). (C) Binding of NP-specific IgH_{V1-72}Igλ monoclonal antibodies that show mitochondrial HEp-2 cell patterns (red lines) to the recombinant protein pML-MIT3 at varying concentrations by ELISA. HEp-2-negative monoclonal antibodies (black lines) and mGO53 monoclonal antibody (grey line) served as controls. (D) Summary of HEp-2 cell reactivity of all monoclonal antibodies tested at 100 µg/ml depending on antigen and immunoglobulin genes used. (E-G) Mixed bone marrow chimeras were generated and immunized with NP-OVA. Fourteen days later, draining lymph nodes and spleens were harvested and FRET⁺ (live) GC B cells of indicated donor-derived genotypes were single-cell sorted. IgH and IgL chains were amplified by PCR and sequenced. (E) Experimental scheme. (F) Same as Fig. 1C but HEp-2 reactive antibodies were tested at 1 µg/ml. (G) Pie charts show the types of BCR lesions detected among non-functional GC B cells of indicated genotypes in the live DZ. (A-G) Statistical significance was assessed by Fisher's exact test. (A-D) For NP-OVA experiments, GC B cells of indicated compartments were single-cell sorted from pools of 1-13 mice per experiment (72 mice in total) with 4 to 9 independent experiments per compartment and each experiment contributing between 1 and 33 antibodies per pie. 30 IgH Igκ antibodies were cloned and expressed from apoptotic DZ GC B cells that were single-cell sorted from a pool of 10 NP-OVA immunized mice. For GT1.1 experiments, GC B cells of indicated compartments were single-cell sorted from pools of 7-10 mice per experiment (41 mice in total) with 4 to 5 independent experiments per compartment and each experiment contributing between 3 and 22 antibodies per pie. (E-G) For mixed bone marrow chimera experiments, GC B cells of indicated compartments and genotypes were single-cell sorted from pools of 10 mice per experiment (40 mice in total) with 2-4 independent experiments per compartment and each experiment contributing between (F) 3 and 41 antibodies or (G) 2 and 34 sequences per pie.

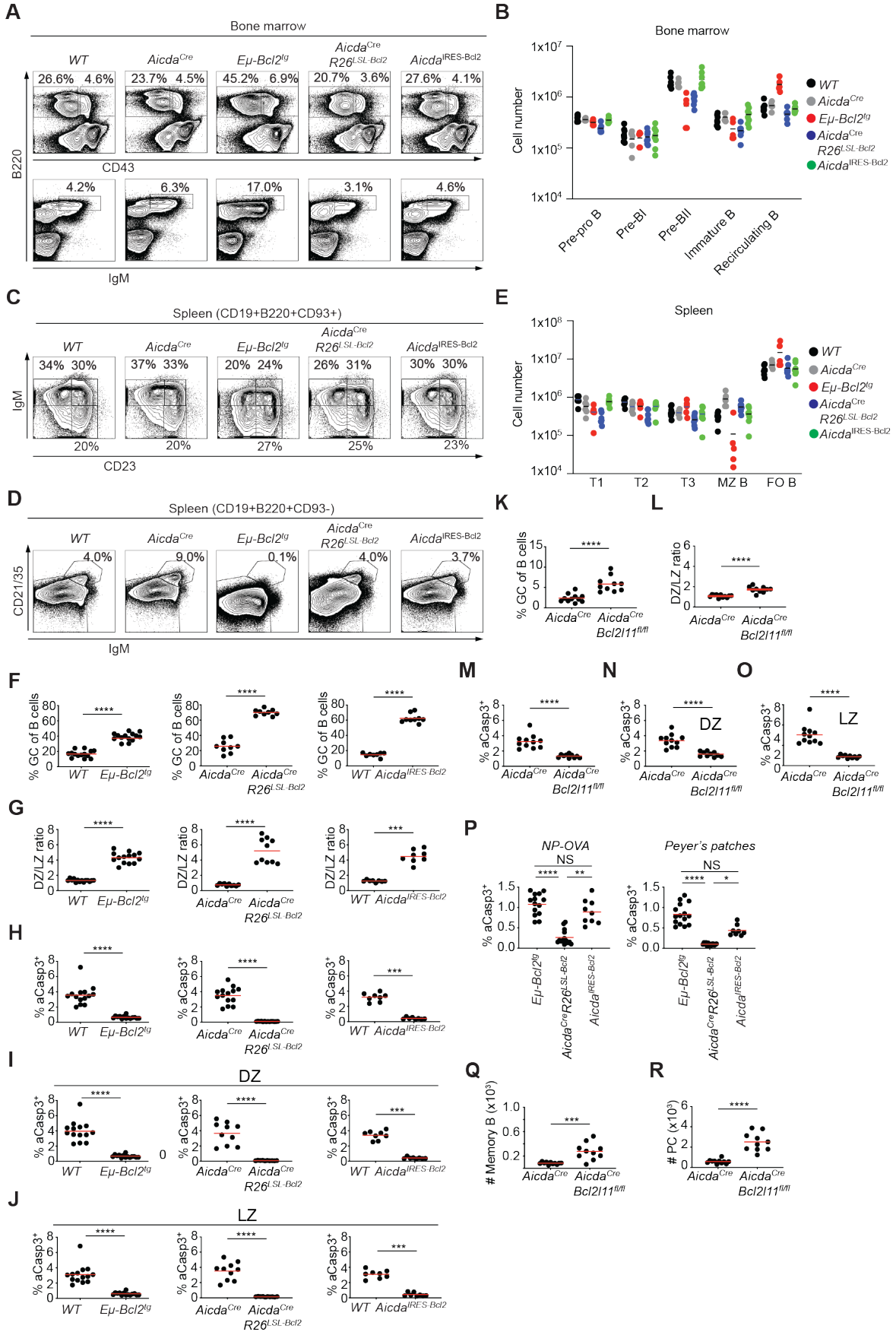


Fig. S2. Characterization of mouse strains with deregulated B cell apoptosis

(A-E) B cell development in mice of the indicated genotypes. (A) Representative flow cytometry plots display CD43 vs. B220 (top) or IgM vs. B220 expression (bottom) among bone marrow cells. (B) Cell numbers of the indicated B cell populations in the bone marrow. (C, D) Representative flow cytometry plots display (C) CD23 vs. IgM and (D) IgM vs. CD21/CD35 expression among indicated splenic B cell gates. (E) Cell numbers of transitional (T1-3), marginal zone (MZ) and follicular (FO) B cells. (F-J) Same as Fig.2B-F but assessing GC B cells in Peyer's patches. (K-O) Same as Fig.2B-F but assessing lymph nodes of NP-OVA immunized *Aicda^{Cre}* and *Aicda^{Cre}Bcl2l1^{fl/fl}* mice. (P) Direct comparison of GC B cell aCasp3 levels among indicated strains in lymph nodes (NP-OVA) or Peyer's patches. (Q, R) Numbers of (Q) lymph node memory B cells and (R) Peyer's patch plasma cells. All results are from 2-3 independent experiments. *** p=0.0002 (F-J), *** p=0.0005 (R), **** p<0.0001 (F-O, R; Mann Whitney test). * p=0.037, ** p=0.003, **** p<0.0001 (P; Kruskal Wallis test with Dunn's multiple comparison test).

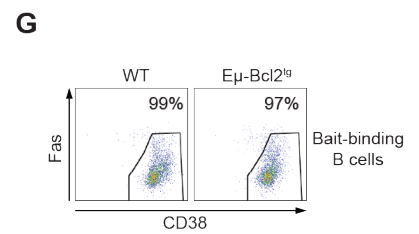
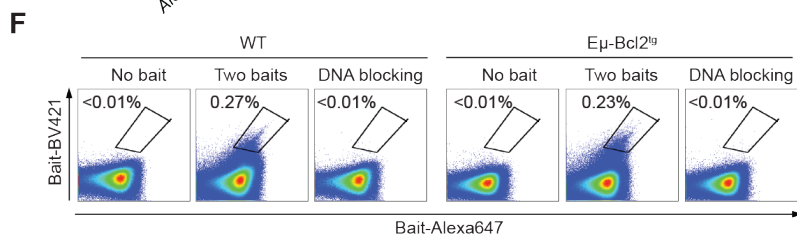
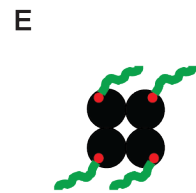
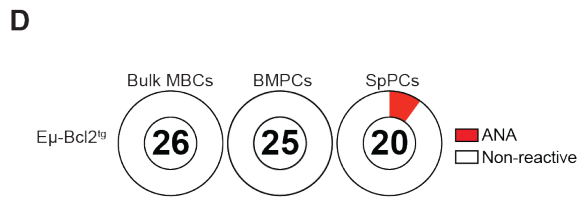
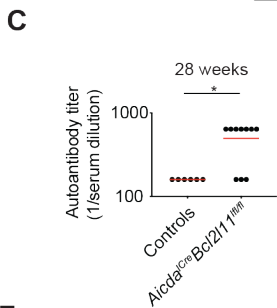
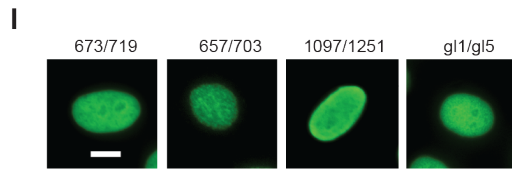
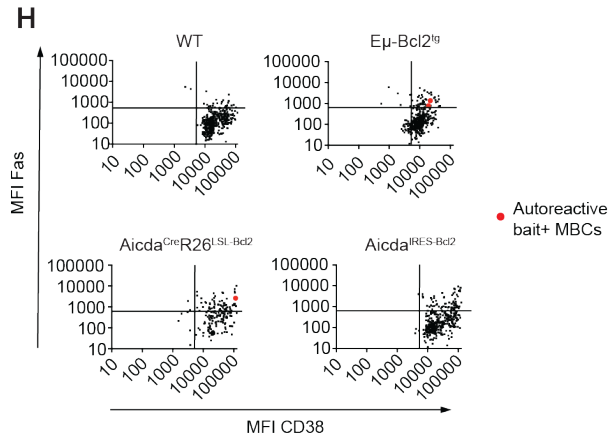
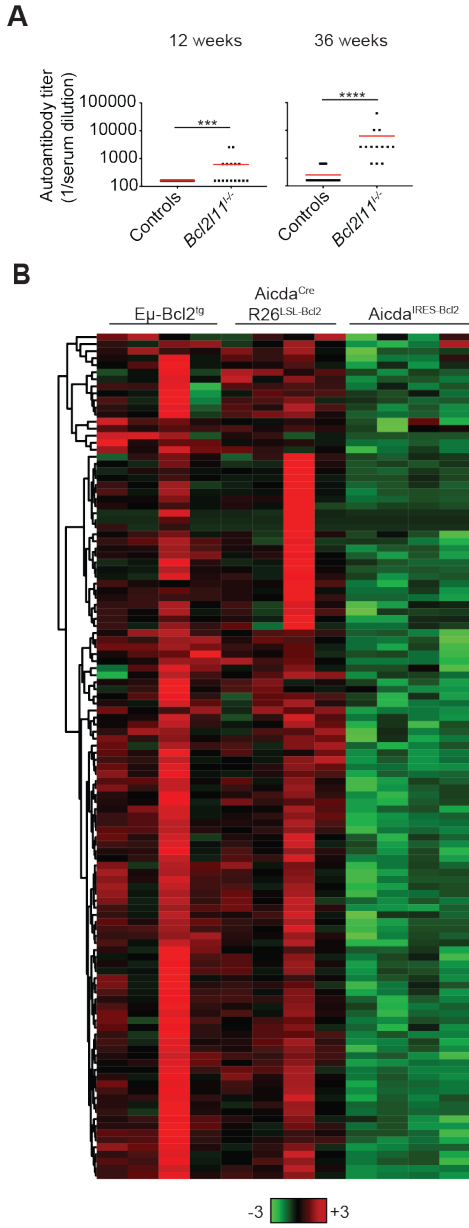


Fig. S3. Control of autoreactive plasma cells and memory B cells by apoptosis

Cohorts of E_{μ} - $Bcl2^{tg}$, $Aicda^{Cre}R26^{LSL-Bcl2}$, $Aicda^{RES-Bcl2}$, $Bcl2l11^{-/-}$ and control mice were monitored over time. (A) End point titers of serum tested for HEp-2 cell reactivity at 12 and 36 weeks. Serum was assessed at 1:640 and consecutive four-fold dilutions. Negative reactivity is shown as 1:160. *** $p=0.0005$, **** $p<0.0001$ (Mann Whitney test). (B) Autoantigen array. Heatmaps show serum IgG reactivity against a panel of 122 antigens (red: strong reactivity; green: low reactivity). Four mice were tested for each genotype. (C) As in (A) but using $Aicda^{Cre}Bcl2l11^{fl/fl}$ mice. * $p=0.011$ (Mann Whitney test). (D-I) Spleen plasma cells (SpPCs), bone marrow plasma cells (BMPCs), IgD⁻ IgM⁻ memory B cells (bulk MBCs) and dsDNA bait-binding memory B cells (bait⁺ MBCs) were single-cell sorted from aged mice of the indicated genotypes. After cDNA preparation, IgH / IgL pairs were PCR amplified, cloned, and monoclonal antibodies were produced and tested for HEp-2 cell reactivity. (D) Pie charts summarize HEp-2 cell reactivity. Antibodies that show antinuclear reactivity at 1 μ g/ml are shown in red. The number in the center of each pie represents the total number of antibodies tested. All antibodies were cloned from the same mouse to compare autoreactivity among the different compartments (E) Schematic of the dsDNA bait. (F-H) Splenocytes of indicated genotypes were stained with fluorochrome-conjugated antibodies and mixtures of Alexa647- and BV421-conjugated dsDNA baits followed by FACS sorting. (F) Representative plots show Alexa647 vs. BV421 fluorescence (two baits) among CD19⁺ B cells. Some samples were incubated with 100 μ g/ml salmon sperm DNA prior to dsDNA bait staining (DNA blocking) or were not incubated with any bait (no bait). Numbers indicated the frequencies of B cells stained by both dsDNA baits. (G) dsDNA bait⁺ B cells were gated and evaluated for CD38 and Fas expression. (H) Index sorting analysis of single dsDNA bait⁺ B cells depicts mean fluorescence intensities for CD38 and Fas staining. Autoreactive cells identified after antibody cloning and expression all show a CD38^{hi} MBC phenotype (red dots). (I) HEp-2 cell fluorescence pattern of the indicated monoclonal antibodies and their common germline revertant g11/g15 (scale bar, 10 μ m). All results are from three independent cohorts of mice and at least two independent sorts for each genotype.

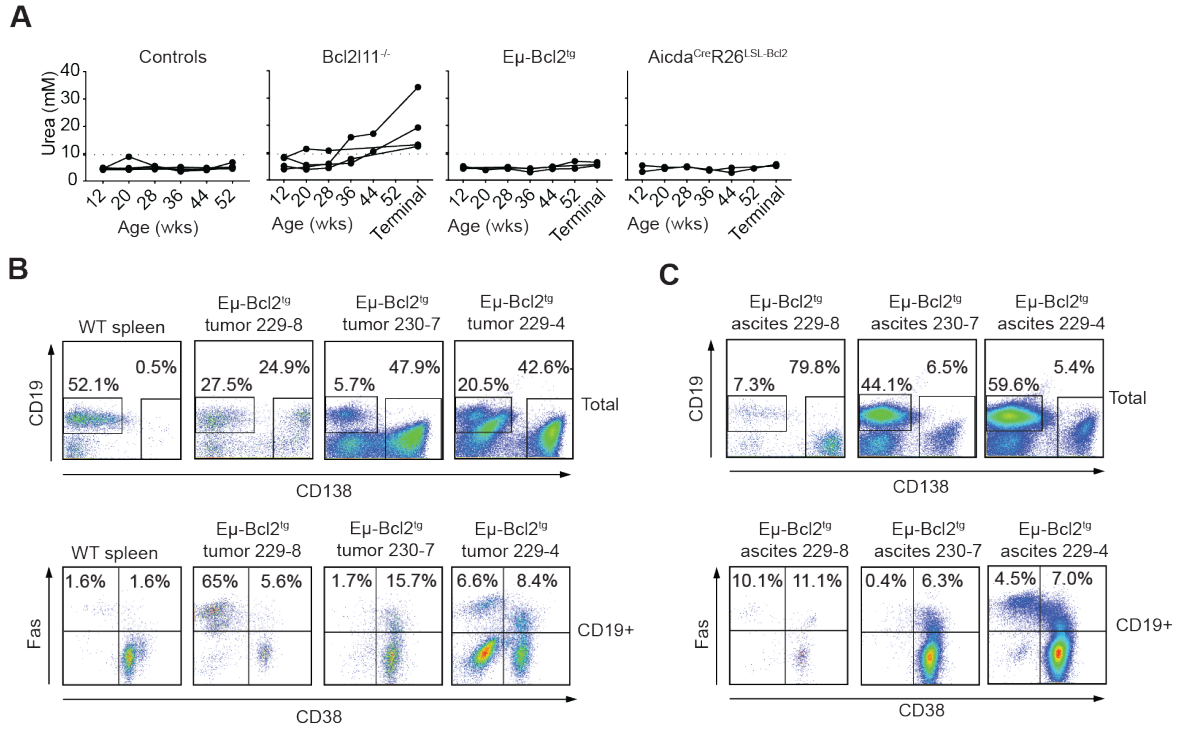


Fig. S4. Kidney function and B cell lymphoma phenotyping

Cohorts of $E\mu\text{-Bcl}2^{tg}$, $Aicda^{CreR26^{LSL-Bcl2}}$, $Bcl2l11^{-/-}$ and control mice were monitored over time. (A) Serum urea concentration at indicated time points. A dotted line is set at the 2-fold mean of control mice. (B, C) Tumors from terminally diseased mice were examined by flow cytometry. Flow cytometry analysis of single cell suspensions from (B) intestinal tumors and (C) ascites fluid. WT spleen served as a control. (A-C) Mice were from at least three independent cohorts.

Data S1. Autoantigen arrays. Net fluorescence intensity (NFI), signal to noise ratio (SNR) and autoantibody score (Ab-score) for each antigen and mouse serum tested.

Data S2. Summary of autoantibody features

Data S3. Summary of pathology findings